UNIVERSITY OF THE PHILIPPINES

RADIOFREQUENCY MAPPING OF AN OMNIDIRECTIONAL ANTENNA IN AN OUTDOOR DISTRIBUTED ANTENNA SYSTEM

By

MAYNETH VINCE R. OFTANA

A Special Problem Submitted to the
Department of Physical Sciences and Mathematics
College of Arts and Sciences
University of the Philippines Manila
Ermita, Manila

In Partial Fulfillment of the Requirements
For the Degree of
Bachelor of Science in Applied Physics

June 2015

Radiofrequency Mapping of an Omnidirectional Antenna in an Outdoor Distributed Antenna System
by Mayneth Vince R. Oftana
Special Problem, Department of Physical Sciences and Mathematics, College of Arts and Sciences
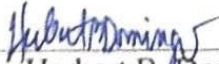University of the Philippines Manila
June 2015

Classification* :   P

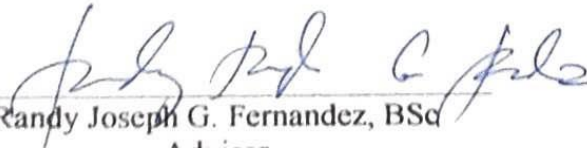* I – invention or creation, P – publication, C – confidential information

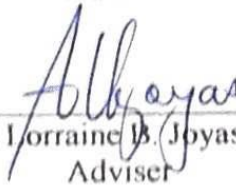|	
Available to the general public	No
Available only after consultation with author/adviser for thesis/dissertation	Yes
Available only to those bound by nondisclosure or confidentiality agreement	Yes

Mayneth Vince R. Oftana
Student

Herbert B. Domingo, MSc
Adviser

Randy Joseph G. Fernandez, BSc
Adviser
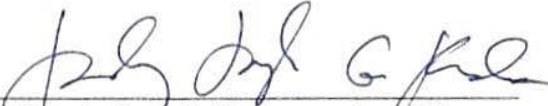
Annie Lorraine B. Joyas, MSc
Adviser

Realyn Joy Uy, MSc
Adviser

ACCEPTANCE SHEET

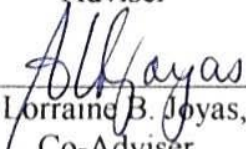The Special Problem entitled "Radiofrequency Mapping of an Omnidirectional Antenna in an Outdoor Distributed Antenna System" prepared and submitted by Mayneth Vince R. Oftana in partial fulfillment of the requirements for the degree of Bachelor of Science in Applied Physics has been examined and is recommended for acceptance.

_____
Herbert B. Domingo, MSc
Adviser

_____
Randy Joseph G. Fernandez, BSc
Adviser

_____
Annie Lorraine B. Joyas, MSc
Co-Adviser
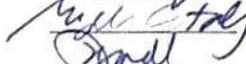
_____
Realyn Joy R. Uy, MSc
Co-Adviser

EXAMINERS:

	Approved	Disapproved
1. Alvin C. Baclig, MSc		
2. Migel Antonio P. Catalig, MSc		
3. Marie Josephine M. De Luna, PhD		
4. Astrid Korina S. Gabo, BSc		
5. Sarah C. Johnson, MSc		
6. Edanjarlo J. Marquez, PhD		
7. William Bill P. Turnbull Jr., MSc		
8. Robert S. Vitancol, MSc		

Accepted and approved as partial fulfillment of the requirements for the degree of Bachelor of Science in Applied Physics.

_____
Herbert B. Domingo, MSc
Unit Head
Physics and Geology Unit
Department of Physical Sciences and
Mathematics

_____
Marcelina B. Lirazan, PhD
Chair
Department of Physical Sciences and
Mathematics

_____
Alex C. Gonzaga, PhD, DrEng
Dean
College of Arts and Sciences

TABLE OF CONTENTS

LIST OF TABLES

Table

LIST OF FIGURES

Figure

LIST OF APPENDICES

Appendix

ACKNOWLEDGEMENT

ABSTRACT

Some members of the general public have safety issues on the sources of non-ionizing radiation found in their environment. This study aims to produce a radiofrequency map to visualize exposure from an omnidirectional antenna in an Outdoor Distributed Antenna System (ODAS). First, field measurements are done in order to obtain the power density levels around the antenna. The highest power density level measured, which is 3.45 mW/m^2, is just 0.07 % of the reference level set by the International Commission on Non-Ionizing Radiation Protection (ICNIRP) for the exposure of the general public to radiofrequency radiation. A map was generated by using Ordinary Kriging as a spatial interpolation method on measured power density values. Cross-validation was done in order to find an optimal search radius to be used in estimating the unknown power densities. Error values were calculated for different search radii, where results show that the error values are lowest at 1m (Mean Absolute Error: 34.13%; Root Mean Squared Error: 44.41%; Mean Absolute Percentage Error: 37.76%). A radiofrequency map was then generated for a search radius of 1m.

PACS

84.40.Ba	Antennas
87.50.sj	Dosimetry/exposure assessment (of radiofrequency and microwave radiation)
84.40.-x	Electromagnetic waves (radiowaves)

CHAPTER 1

INTRODUCTION

Cell sites mounted on towers or on buildings cover large geographic areas with relatively high user capacity. These macrocell sites deliver wireless communication services to their users in the form of voice, text, web and data applications. Since there is a rapid increase in the consumption of the services mentioned, some existing networks could not meet the coverage and capacity demands [1]. To fill in the service gaps, providers are turning to Distributed Antenna System (DAS) solutions to increase the data-handling capacity of networks and to accommodate the growing user traffic.

A DAS is a network of spatially separated antenna nodes connected to a common transport medium [1]. Its primary components include: a number of DAS nodes each with at least one antenna for the transmission and reception of radiofrequency signals, a coaxial/fiber optic cable connecting each node back to a central communications hub site and lastly, radio transceivers to process/control the transmitted signals. It is considered a key technology in the next generation mobile communications (beyond 3G and 4G) since one of its characteristics is that it enables resources to be targeted in areas where it is most needed with respect to the subscribers' changing demand and location [2,3]. In addition to this, with the presence of multiple antennas, there is signal coprocessing and reduction in the users' access distance which contributes to an expanded network capacity. DAS networks are scalable and flexible. It can support the same coverage area as that of traditional cell sites with lower transmitted power [4]. One network can range

from having at least two up to hundreds of DAS Nodes depending on the geographic area to be covered. It can be configured to use multiple wireless technologies across multiple frequency bands in a wide range to accommodate as many users as possible. The typical operating frequency of a neutral host DAS is from 698 to 2700 MHz or wider depending on the service provider [5]. It can be deployed both indoor and outdoor typically in environments with dense urban population. These areas include airports, stadiums, arenas, convention centers, universities, high rise buildings, neighborhoods and even entire cities since these are the locations that require high capacities to offload traffic from constrained cell sites [6].
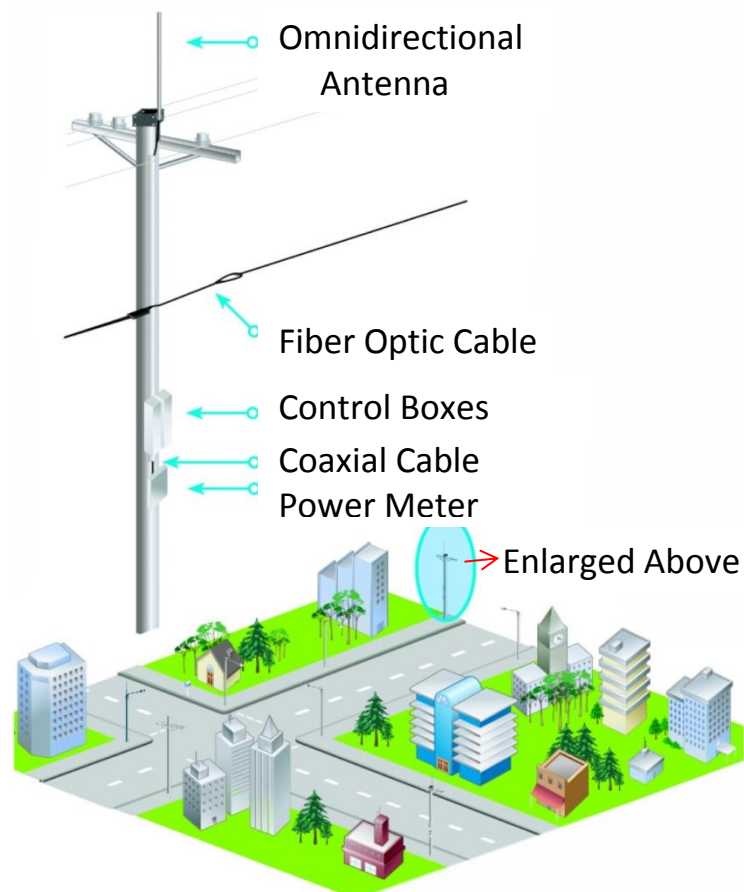
Figure 1.1. An Outdoor Distributed Antenna System in an Urban Area
Adapted from [29]

An Outdoor Distributed Antenna System (ODAS) can support up to 16 frequency bands within half a mile range while supporting 300 simultaneous connections for each node [1]. To reduce the visual impact of outdoor antennas, these are usually attached or disguised as structures in public rights of way like utility poles and street lights at uniform heights as illustrated in Figure 1.2. In the Philippines, the first ODAS was recently installed in 2013 at Dasmariñas Village, Makati. Each street in the said location has at least one antenna disguised as a lamp post that provides coverage within 200-350 m [7].
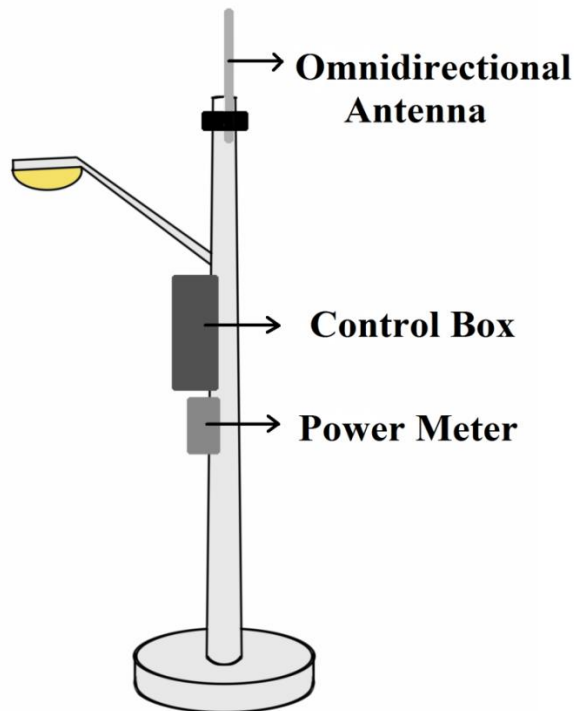
Figure 1.2. A Single Node of an Outdoor Distributed
Antenna System with an Omnidirectional Antenna

Antennas emit signals through electromagnetic waves. Since the expansion of mobile communications, the sources of electromagnetic radiation in the radiofrequency range became closer to the immediate environment of people [8]. Due to media heightened fear and misunderstanding of electromagnetic fields, members of the public sometimes have hypothesized or imagined hazards of radiofrequency radiation exposure that are exacerbated in comparison to the established risks [9]. This gives rise to some safety concerns on non-ionizing radiation.

To determine human exposure to non-ionizing radiation, a radiofrequency map can be used. It is an informative representation of the magnitude of the exposure over an area. This map can be generated from the measured values of the power density. This approach is the most straightforward; however, it is very tedious since it requires a large number of samples obtained through measurement campaigns [10]. Since a continuous dataset is preferable for mapping, it is not feasible to measure the power density at every point within the area of interest. Therefore, a spatial interpolation method will be used. This allows the estimation of unknown values at the non-sampled locations.

In this study, a radiofrequency map for an antenna in an ODAS will be generated. This will be done through interpolating the power density levels obtained from field measurements. Ordinary Kriging will be used as an interpolation method to estimate the values needed for mapping. The measured values will then be assessed for compliance with the existing standards set by the International Commission on Non-Ionizing Radiation Protection (ICNIRP).

1.1 Statement of the Problem

An Outdoor Distributed Antenna System (ODAS) is a new architecture for public wireless access, which refers to a generalized multiple-input multiple-output (MIMO) system comprising an antenna array at one side of the link and several largely separated antenna arrays at the other side [4]. The architecture of an ODAS is flexible and outperforms conventional wireless systems. It is emerging as a promising candidate for future mobile communication systems that are beyond 3G and 4G. Therefore, it meets the users' demands for high data rate communication services with its enhanced signal quality, increased system capacity and improved coverage in densely populated areas.

Along with the recent installment of an ODAS in the Philippines in 2013, some safety concerns arise. Since these systems use antennas mounted on posts located by the sidewalk, there is a concern for exposure to non-ionizing radiation. The goal of this study will be the generation of a radiofrequency map to visualize the exposure from an omnidirectional antenna in an ODAS. This will be obtained by interpolating the measured power density values using Ordinary Kriging. Through this, the safety of the general public will be verified.

1.2 Objectives

- To measure the power density levels of an antenna in an ODAS node.
- To generate a radiofrequency map by using a spatial interpolation technique on the measured power densities.
- To assess the safety of the general public from the radiofrequency radiation emitted by the antenna in a node of an ODAS.

1.2 Significance of the Study

Some members of the public have a negative perception to the exposure to radiofrequency radiation despite the lack of consistent evidence regarding its adverse health effects [11]. Therefore, it is important to assess and communicate the risks of exposure.

Since an ODAS is a relatively new technology in the Philippines, the study would provide information on the radiofrequency radiation from an antenna in this system. This would be beneficial in addressing the concerns on public safety.

1.3 Scope and Limitations

An ODAS is composed of several nodes which may contain one or more antennas. To measure the power density levels around each node for the installment would be very time-consuming. Therefore, it would be more feasible to examine a single antenna for each type, model or frequency band used in the system.

There are omnidirectional and panel antennas operating at frequencies suitable for GSM, UMTS and LTE networks for the ODAS of interest. In this study, a single omnidirectional antenna operating at 870-960 MHz was investigated for its contribution to the radiofrequency radiation exposure of the members of the public.

CHAPTER 2

REVIEW OF RELATED LITERATURE

2.1 Radiofrequency Radiation

Categorizing electromagnetic energy by frequency, radiofrequency is arbitrarily defined to be the part of the electromagnetic spectrum where the frequencies range from 3 kHz to 300 GHz. It has industrial, scientific and medical applications but its most important use is in providing telecommunications services. It is utilized in radio and television broadcasting, mobile telephones, radars and satellite communications [12].

Radiofrequency energy is non-ionizing radiation (NIR). Before the end of World War II, safety practices to control the hazards from NIR only received a little attention. With the post-war boom in electronics and communications, attention was focused on its possible health effects to the public [13]. Now, there are several organizations and government agencies that have developed guidelines and safety standards for radiofrequency radiation. This includes the International Commission on Non-Ionizing Radiation Protection (ICNIRP) which is an independent scientific organization that has set restrictions for occupational and general public exposures.

Radiofrequency waves contain both an electric and magnetic component. One unit that can characterize electromagnetic fields is the power density. It is the intensity of the electromagnetic wave (expressed in W/m^2) that could be used to define the guidelines for exposure to radiofrequency radiation.

Table 2.1. Reference levels for occupational exposure to time-varying electric and magnetic fields (unperturbed rms values). Adapted from [21]

Frequency range	E-field strength $(V\,m^{-1})$	H-field strength $(A\,m^{-1})$	B-field (μT)	Equivalent plane wave power density S_{eq} $(W\,m^{-2})$
up to 1 Hz	—	1.63×10^5	2×10^5	—
1–8 Hz	20,000	$1.63 \times 10^5/f^2$	$2 \times 10^5/f^2$	—
8–25 Hz	20,000	$2 \times 10^4/f$	$2.5 \times 10^4/f$	—
0.025–0.82 kHz	$500/f$	$20/f$	$25/f$	—
0.82–65 kHz	610	24.4	30.7	—
0.065–1 MHz	610	$1.6/f$	$2.0/f$	—
1–10 MHz	$610/f$	$1.6/f$	$2.0/f$	—
10–400 MHz	61	0.16	0.2	10
400–2,000 MHz	$3f^{1/2}$	$0.008f^{1/2}$	$0.01f^{1/2}$	$f/40$
2–300 GHz	137	0.36	0.45	50

[a] Note:
1. f as indicated in the frequency range column.
2. Provided that basic restrictions are met and adverse indirect effects can be excluded, field strength values can be exceeded.
3. For frequencies between 100 kHz and 10 GHz, S_{eq}, E^2, H^2, and B^2 are to be averaged over any 6-min period.
4. For peak values at frequencies up to 100 kHz see Table 4, note 3.
5. For peak values at frequencies exceeding 100 kHz see Figs. 1 and 2. Between 100 kHz and 10 MHz, peak values for the field strengths are obtained by interpolation from the 1.5-fold peak at 100 kHz to the 32-fold peak at 10 MHz. For frequencies exceeding 10 MHz it is suggested that the peak equivalent plane wave power density, as averaged over the pulse width, does not exceed 1,000 times the S_{eq} restrictions, or that the field strength does not exceed 32 times the field strength exposure levels given in the table.
6. For frequencies exceeding 10 GHz, S_{eq}, E^2, H^2, and B^2 are to be averaged over any $68/f^{1.05}$-min period (f in GHz).
7. No E-field value is provided for frequencies <1 Hz, which are effectively static electric fields. Electric shock from low impedance sources is prevented by established electrical safety procedures for such equipment.

Table 2.2. Reference levels for general public exposure to time-varying electric and magnetic fields (unperturbed rms values). Adapted from [21]

Frequency range	E-field strength $(V\,m^{-1})$	H-field strength $(A\,m^{-1})$	B-field (μT)	Equivalent plane wave power density S_{eq} $(W\,m^{-2})$
up to 1 Hz	—	3.2×10^4	4×10^4	—
1–8 Hz	10,000	$3.2 \times 10^4/f^2$	$4 \times 10^4/f^2$	—
8–25 Hz	10,000	$4,000/f$	$5,000/f$	—
0.025–0.8 kHz	$250/f$	$4/f$	$5/f$	—
0.8–3 kHz	$250/f$	5	6.25	—
3–150 kHz	87	5	6.25	—
0.15–1 MHz	87	$0.73/f$	$0.92/f$	—
1–10 MHz	$87/f^{1/2}$	$0.73/f$	$0.92/f$	—
10–400 MHz	28	0.073	0.092	2
400–2,000 MHz	$1.375f^{1/2}$	$0.0037f^{1/2}$	$0.0046f^{1/2}$	$f/200$
2–300 GHz	61	0.16	0.20	10

[a] Note:
1. f as indicated in the frequency range column.
2. Provided that basic restrictions are met and adverse indirect effects can be excluded, field strength values can be exceeded.
3. For frequencies between 100 kHz and 10 GHz, S_{eq}, E^2, H^2, and B^2 are to averaged over any 6-min period.
4. For peak values at frequencies up to 100 kHz see Table 4, note 3.
5. For peak values at frequencies exceeding 100 kHz see Figs. 1 and 2. Between 100 kHz and 10 MHz, peak values for the field strengths are obtained by interpolation from the 1.5-fold peak at 100 kHz to the 32-fold peak at 10 MHz. For frequencies exceeding 10 MHz it is suggested that the peak equivalent plane wave power density, as averaged over the pulse width does not exceed 1,000 times the S_{eq} restrictions, or that the field strength does not exceed 32 times the field strength exposure levels given in the table.
6. For frequencies exceeding 10 GHz, S_{eq}, E^2, H^2, and B^2 are to be averaged over any $68/f^{1.05}$-min period (f in GHz).
7. No E-field value is provided for frequencies <1 Hz, which are effectively static electric fields. perception of surface electric charges will not occur at field strengths less than 25 kVm^{-1}. Spark discharges causing stress or annoyance should be avoided.

The biological effects of radiofrequency radiation are frequency dependent and could be grouped into electrostimulatory effects (3 kHz – 5 MHz) and thermal effects (100 kHz – 3 GHz). An electrostimulatory effect is the generation of painful nerve impulses due to an electric field at high levels. The thermal effects on the other hand are caused by exposure to very high levels of RFR that results in rapid heating of the biological tissue which could be localized or affecting the whole body [13]. At levels lower than what produces significant heating, the evidence for detrimental biological effects is ambiguous and unproven. Further research is needed for these "nonthermal" effects [12].

2.2 Spatial Interpolation

Spatial interpolation refers to the procedure of predicting the values of the target variable over a whole area of interest [14]. Since it assumes that the data is continuous over space, it is typically used in producing images or maps.

Interpolation techniques can be deterministic or geostatistical [15]. Deterministic interpolation creates surfaces from known data values based on the extent of similarity or the degree of smoothing. Geostatistical techniques, on the other hand, incorporate the statistical properties of the measured points.

Geostatistics includes several methods that use kriging [16]. Kriging is a term for a family of generalized least-squares regression algorithms that provide the best linear unbiased predictions. It is an interpolation technique widely applied in different fields since it can predict values without bias, determine the best estimator of the variable and calculate the accuracy of the interpolation by calculating the error estimate (kriging

variance) together with the interpolated values [17]. It is already used in the context of electromagnetic field mapping [17,19].

In order to apply kriging interpolation, the experimental semivariogram of the data must be acquired first. After that, it must be fitted into a theoretical semivariogram model before estimations can be made.

2.2.1 Semivariogram Estimation and Modelling

The semivariance (γ) between two data points is defined as

$$\gamma(x_i, x_0) = \gamma(h) = \frac{1}{2}var[Z(x_i) - Z(x_0)], \tag{1}$$

where h is the distance between x_i and x_0 and $\gamma(h)$ is the semivariogram (also referred to as the variogram). The semivariogram is a graph showing the semivariance as a function of separation distances or "lags" [16]. This is important since it indicates the degree of spatial correlation in the measurements at the sample locations [18].
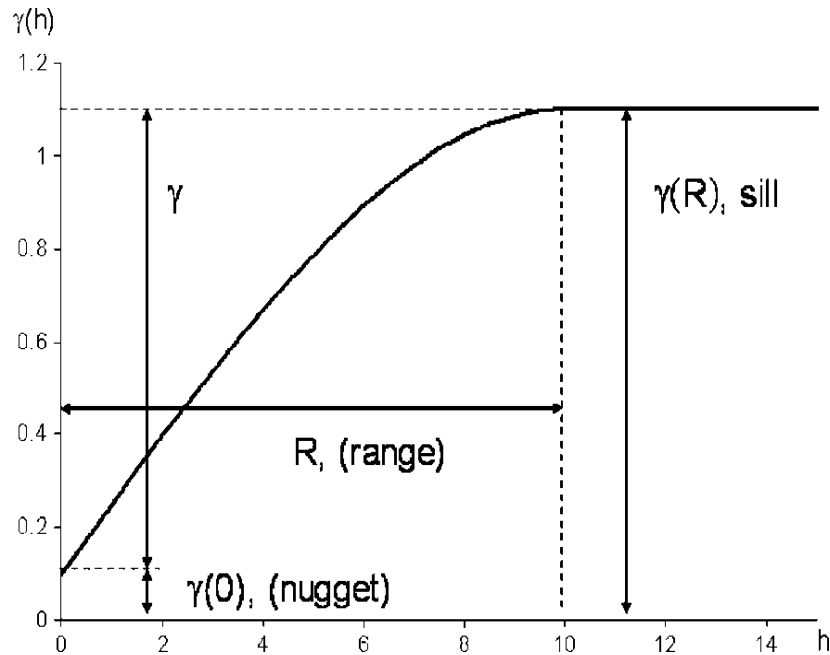
Figure 2.1. An example of a theoretical semivariogram showing the range (R),
the nugget (C_0) and the sill ($C_0 + C_1$). Adapted from [19]

The semivariogram has several important features: the nugget, the range and the sill as seen on Figure 2.1. The nugget reflects the variance of sampling errors and the microvariance (the variance at distances shorter than the minimum distance between the samples) [16,18]. The range is the distance at which the sill or the maximum variance is reached. Spatial independence is observed for samples that are separated with a distance larger than range.

The semivariance can be estimated from the measured data as follows:

$$\hat{\gamma}(h) = \frac{1}{2n} \sum_{i=1}^{n} [z(x_i) - z(x_i + h)]^2, \tag{2}$$

where n is the number of the pairs of sample points separated by the lag distance h. The graph of $\hat{\gamma}(h)$ versus h is known as the experimental semivariogram [16]. Obtaining this is the first step in the variographic analysis.

The next step following the estimation of the experimental semivariogram is fitting it into a theoretical model. A smooth curve is fit to the experimental values to obtain a mathematical expression that can describe the variance and ignore the erratic fluctuations in the data [20]. The popular models for semivariograms are shown in Figure 2.2.
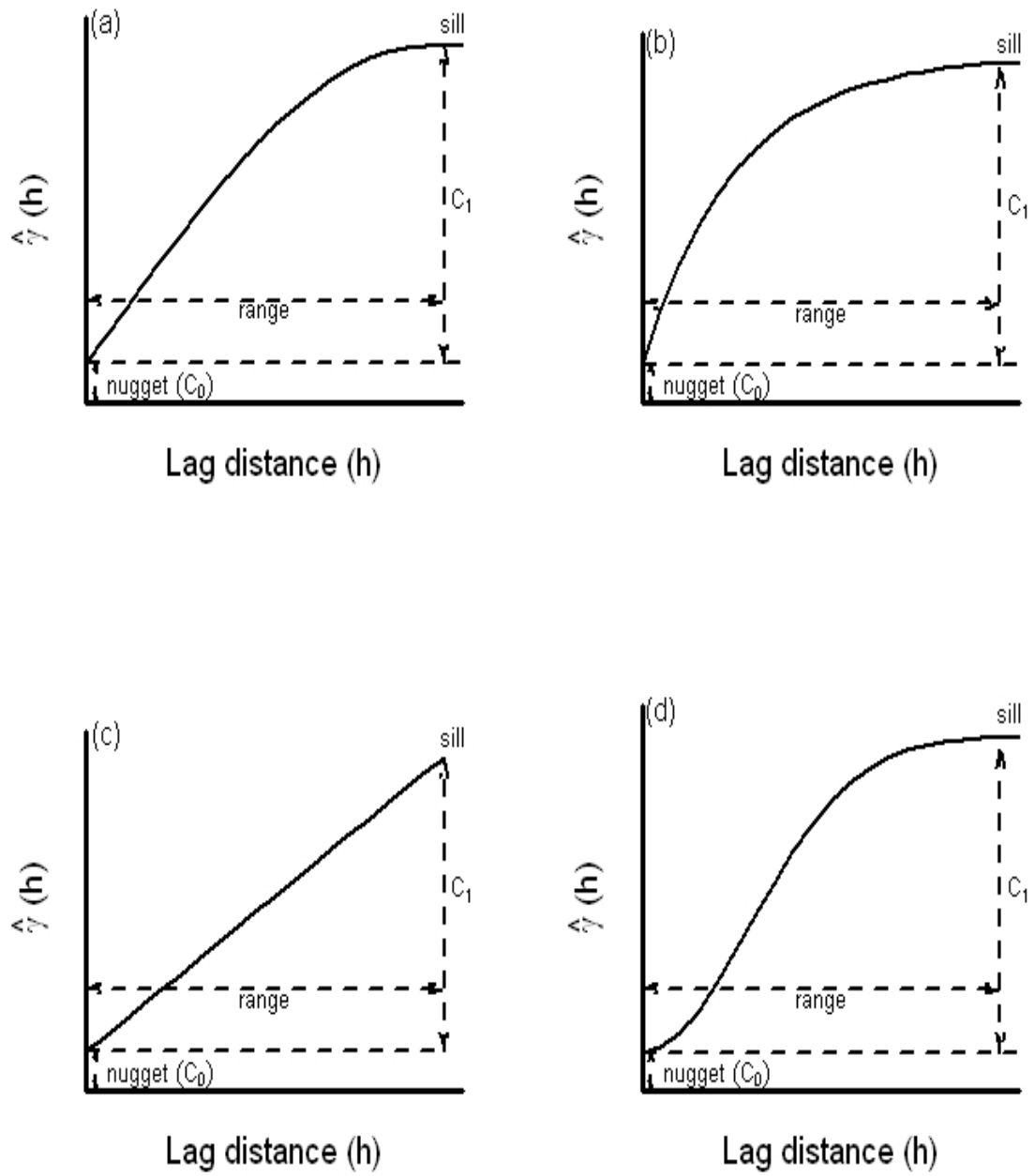
Figure 2.2. Commonly Used Variogram Models. (a) Spherical;

(b) Exponential; (c) Linear; (d) Gaussian. Adapted from [16]

2.2.2 <u>Ordinary Kriging</u>

In Ordinary Kriging, the value at an unsampled location is interpolated based on the available data from its surrounding points. If $z(x_i)$, $i = 1,2, \dots, N$ are the measured values of z at points $x_1, x_2, \dots, x_N$ (in two dimensions $x_i \equiv \{x_{i1}, x_{i2}\}^T$), the value of Z located at a new point x_0 can be interpolated by

$$\hat{Z}(x_0) = \sum_{i=1}^{n} \lambda_i \, z(x_i), \tag{3}$$

where $\lambda_i, i = 1,2, \dots N$ are the kriging weights. These are obtained by minimizing the prediction error variance through the following set of equations

$$\sum_{i=1}^{n} \lambda_i \, \gamma(x_i - x_j) + \psi(x_0) = \gamma(x_j - x_0) \, for \, all \, j \tag{4}$$

$$\sum_{i=1}^{n} \lambda_i = 1. \tag{5}$$

$\gamma(x_i - x_j)$ is the semivariance between points i and j, $\gamma(x_j - x_0)$ is the semivariance between point j and the interpolant x_0 and $\psi(x_0)$ is a lagrange multiplier.

The weights are a decreasing function of distance. Since the surrounding known points are used to estimate the value at an unknown point, a neighborhood or a search radius could be specified around the point to be interpolated. This determines the values to be included for the interpolation. In Ordinary Kriging, the radius of the neighborhood can be specified. Observed values that are within the radius are used for the interpolation.

CHAPTER 3

MATERIALS AND METHODS

The flow of the methodology is illustrated in Figure 3.1. It is generally divided into the field measurement of the power density and the interpolation of the measured values in order to construct a map.
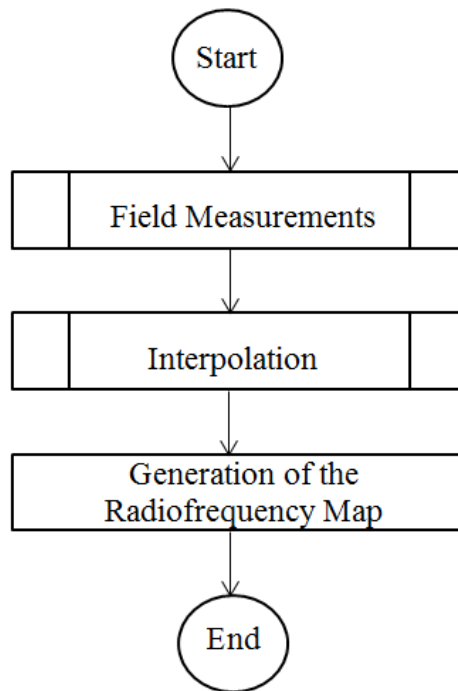
Figure 3.1. The Flowchart for the Methodology

3.1 Field Measurement

Site Description: The ODAS installment is located at Dasmariñas Village. In urban areas, there are several obstructions which may impede the procedures for the data gathering. The presence of several objects especially metallic ones can cause the reflection of radiofrequency fields. Thus, the antenna node measured shown in Figure 3.2 was at a corner road due to the absence of cars parked within the vicinity. The lamp post where the antenna is mounted is approximately 10 m in height.
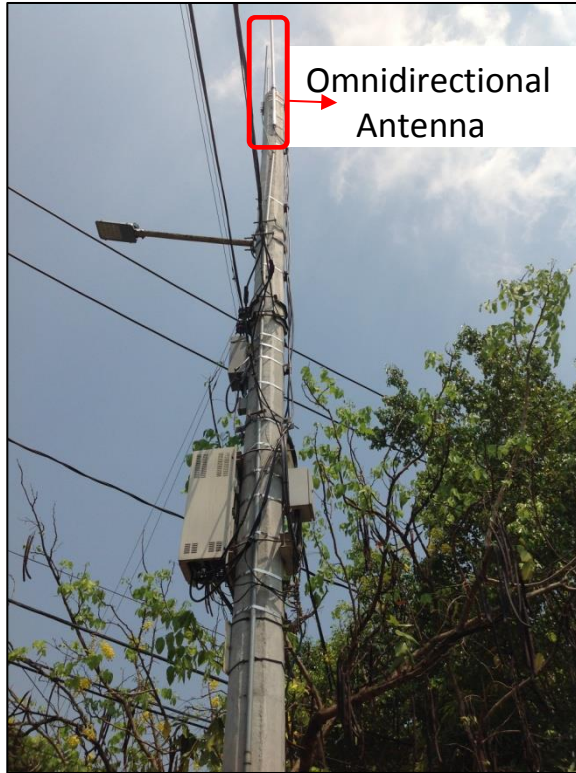
Figure 3.2. The Actual Antenna Node located at Santan corner Dasmariñas St.

Figure 3.3. The Model of the Omnidirectional Antenna. Adapted From [28]

A Selective Radiation Meter (SRM-3000, Narda Safety Test Solutions) was utilized in this study. It is used to measure high frequency fields from 100 kHz - 3 GHz [30]. The Narda SRM-3000 is consisted of a basic unit and a measuring antenna. The measuring antenna is a three axis antenna designed for taking isotropic (non-directional) measurements in outdoor locations. It was mounted on a wooden tripod at a height of 1.5 m considering that this is the average height of a human being. An RF cable connects the triaxial antenna and the basic unit as illustrated in Figure 3.4.
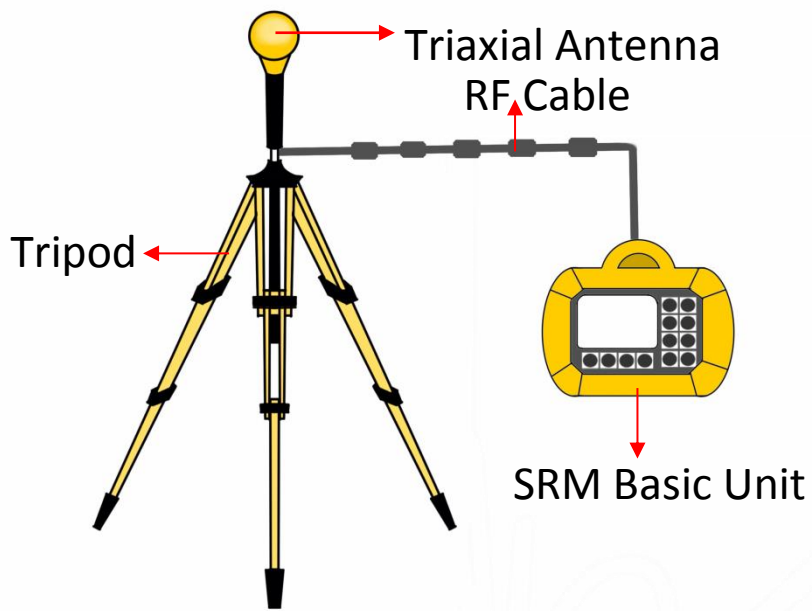
Figure 3.4. The set-up for the measuring equipment

The time analysis mode of the SRM was used to measure the averaged exposure levels. The frequencies measured for this setting are user-defined. Therefore, the field strength values are measured between 870 to 960 MHz since this is the frequency band of the omnidirectional antenna of interest. Each measurement at a single point is averaged over a period of 6 minutes. This duration of 6 minutes is the averaging time also known as the 'thermal time constant' according to the standards for non-ionizing radiation [21].

The sampling pattern is shown in Figure 3.5. There are several other sampling patterns [22]. However, a regular grid is used here for practical purposes. Markers are placed per measurement point to speed up the process of data-gathering. The field strength in terms of the power density was measured at the points indicated.

WALL

SIDE WALK
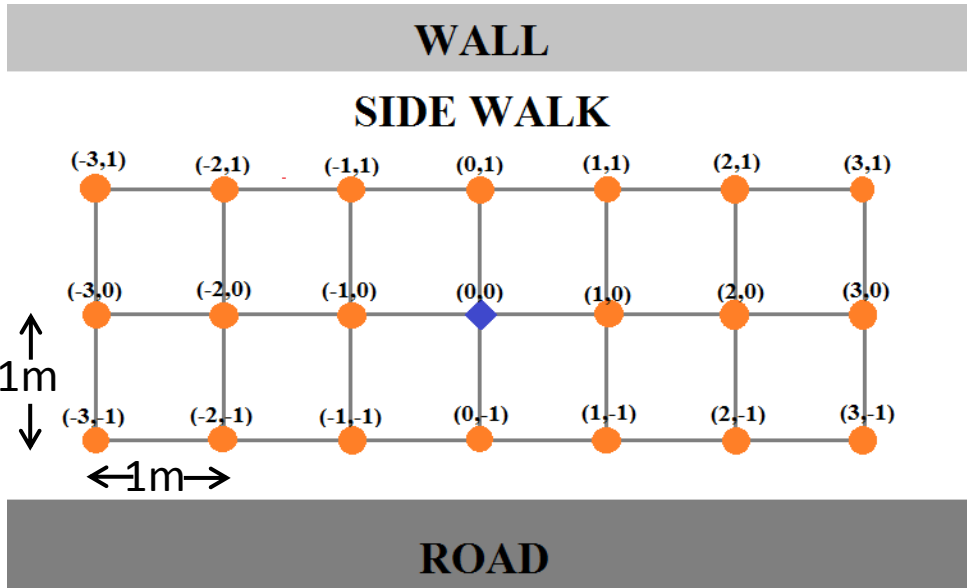
Figure 3.5. The antenna to be measured in this sampling pattern is at the origin. The sampling points (marked as the orange dots) are at a distance of 1 m away from each other

Figure 3.6. Photo During the Field Measurements

3.2 Ordinary Kriging

There is a total of 20 sample points around the antenna where the power density was obtained. The method to interpolate the values needed for mapping was essentially divided into three parts: obtaining the experimental variogram, fitting it into a theoretical model and the estimation of the unknown values. This was performed in Matlab by utilizing the functions included in James Ramm's "Kriging and Inverse Distance Interpolation Using Gstat" zip file and Wolfgang Schwanghart's "Variogramfit" function [25,26]. The script file made is found in the Appendix 5. Comments are imbedded in the script file for more details.

The experimental semivariances are computed for the lag intervals of 1 m, 2 m, 3 m, 4 m, 5 m, 6 m and 7 m. These values are plotted as the experimental variogram. In order to obtain a function, a theoretical model is fitted to this experimental semivariogram. A linear model was used and its performance in predicting the actual values of the power density was evaluated. This was determined by cross-validation. Cross-validation is done by eliminating the value at a point, estimating the value at that location using the remaining data and then computing the difference for the actual and the estimated value for each data location [23]. Several error measurements could be used to determine the accuracy and the precision of spatial interpolation methods in general [16] [24]. The difference of the estimated from the actual power density will be examined using the Mean Absolute Error (MAE), Root Mean Squared Error (RMSE) and the Mean Absolute Percentage Error (MAPE). The formulas for the ME, RMSE and the MAPE are as follows:

$$MAE = \frac{1}{N}\sum_{i=1}^{N} |z(x_i) - \hat{z}(x_i)| \tag{7}$$

$$RMSE = \sqrt{\frac{1}{N}\sum_{i=1}^{N} \{z(x_i) - \hat{z}(x_i)\}^2} \tag{8}$$

$$MAPE = \frac{1}{N}\sum_{i=1}^{N} \frac{|z(x_i) - \hat{z}(x_i)|}{z(x_i)} \tag{9}$$

where N is the number of values in the data set, $z(x_i)$ is the observed value and $\hat{z}(x_i)$ is the interpolated values. The errors were computed at different search radii of 1 m, 2 m, 3 m, 4m, 5m and 6m. The biggest search radius is 6 m since the largest diagonal distance between two points in the grid is 6.32 m. The radius for which the error percentages are the lowest is used to interpolate the values needed for the generation of the radiofrequency map.

CHAPTER 4

RESULTS AND DISCUSSION

The values measured for the power density around the antenna node sorted from lowest to highest and is shown in Figure 4.1. The minimum value obtained is $0.2896 \frac{mW}{m^2}$ while the maximum is $3.45 \frac{mW}{m^2}$.
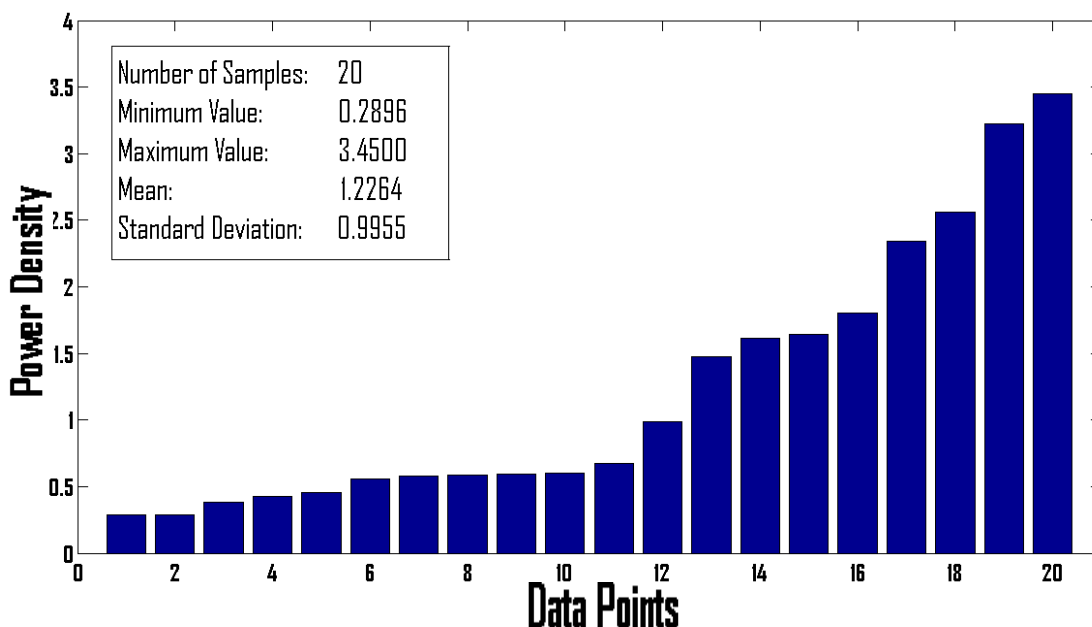
Figure 4.1. The Power Density Values Measured in $\frac{mW}{m^2}$

The frequency range of the measured omnidirectional antenna (870-960 MHz) is between 400-2,000 MHz. According to the ICNIRP, the reference level for the exposure of the general public to the radiofrequency radiation emitted by sources operating in this range is

$$\frac{f}{200} \frac{W}{m^2} . \tag{14}$$

Therefore, the exposure limit is

$$\frac{960}{200} \frac{W}{m^2} = 4.8 \frac{W}{m^2} = 4800 \frac{mW}{m^2} . \tag{15}$$

The highest value measured for the power density which is 3.45 $\frac{mW}{m^2}$ is just 0.07 % of the limit set by the ICNIRP.
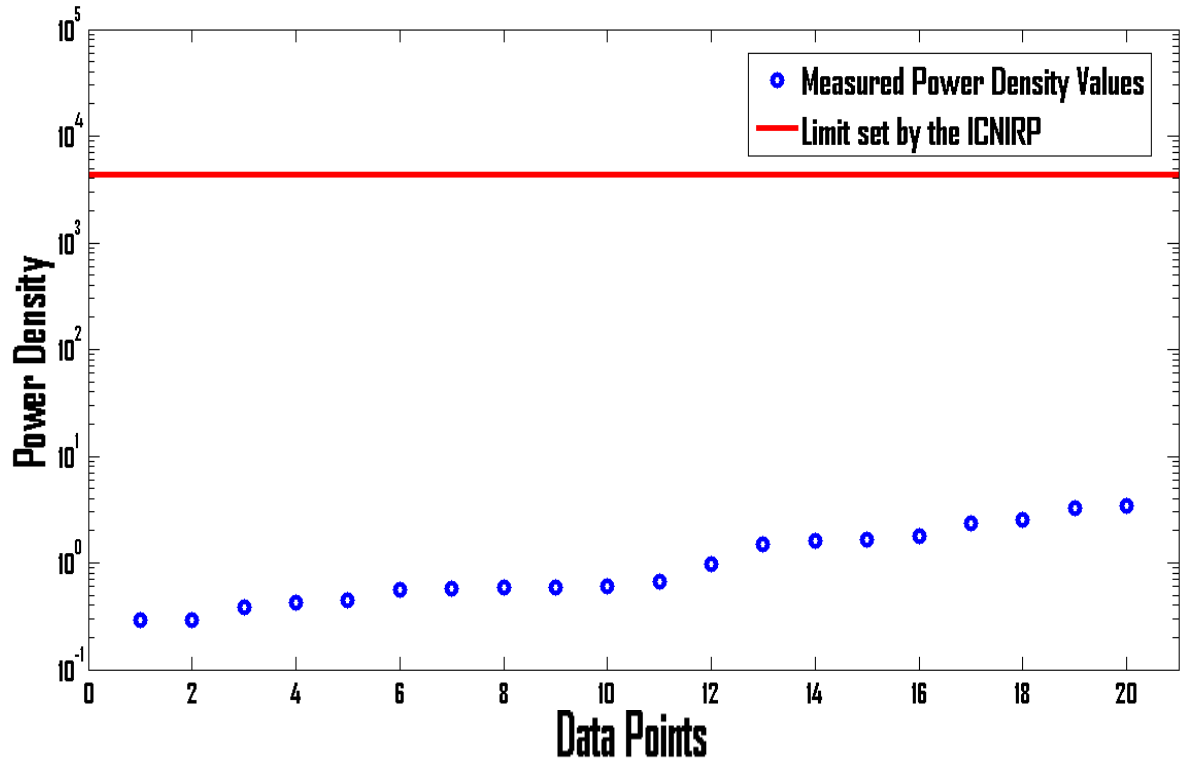
Figure 4.2. Comparison of the Measured Power Density Values and
the limit set by the ICNIRP in $\frac{mW}{m^2}$

The semivariances are computed in matlab. When plotted, these correspond to the experimental variogram. The function obtained by fitting the variogram into a linear model shown in Figure 4.3 is

$$\gamma(h) = 1.9236 \left(\frac{h}{5.3507}\right), \ where\ h\ is\ the\ separation\ distance \qquad (12)$$

$$R^2: \qquad\qquad 0.9980 \qquad\qquad (13)$$
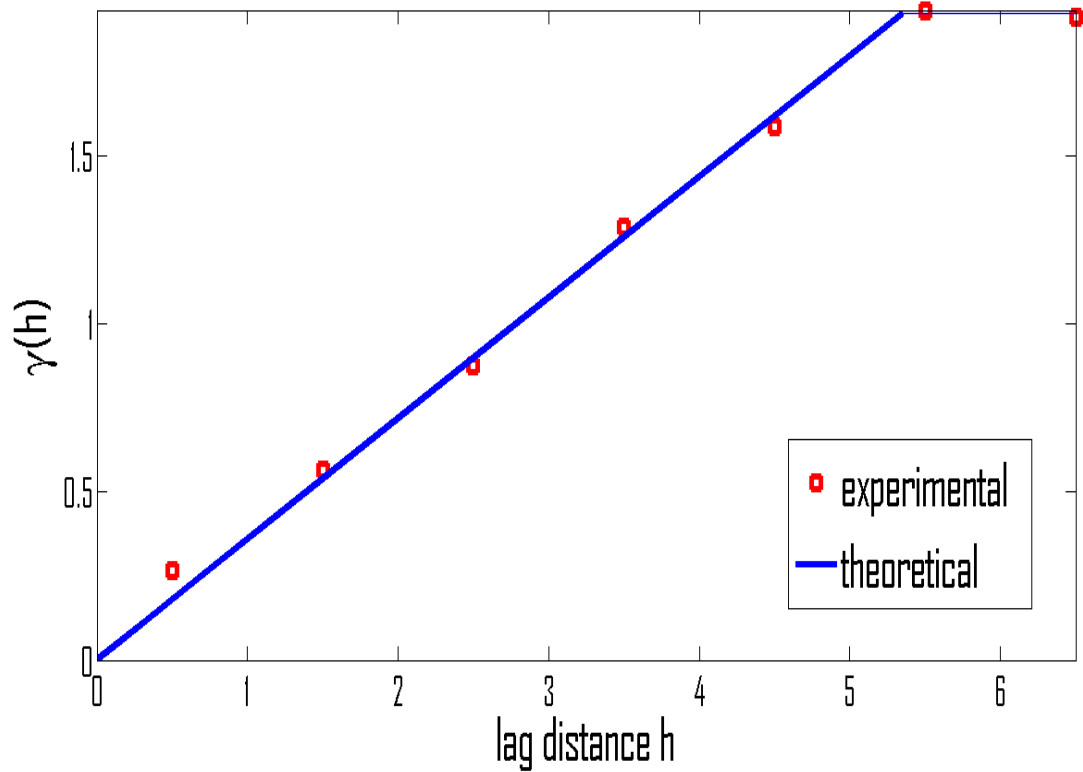
Figure 4.3. The Experimental Semivariogram
with a Fitted Theoretical Linear Model

Observing the coefficient of determination R^2 for the linear model in Equation 13, it can be observed that it provides a good fit to the semivariances computed from the measured values. After checking the goodness of fit, cross validation was performed in order to determine the optimal search radius for interpolation. One measured data is removed from the set and its value was estimated using its neighbors within varying distances for the radius. This was done for all 20 data points. The MAE, RMSE and the MAPE are shown in Figure 4.4, Figure 4.5 and Figure 4.6, respectively.
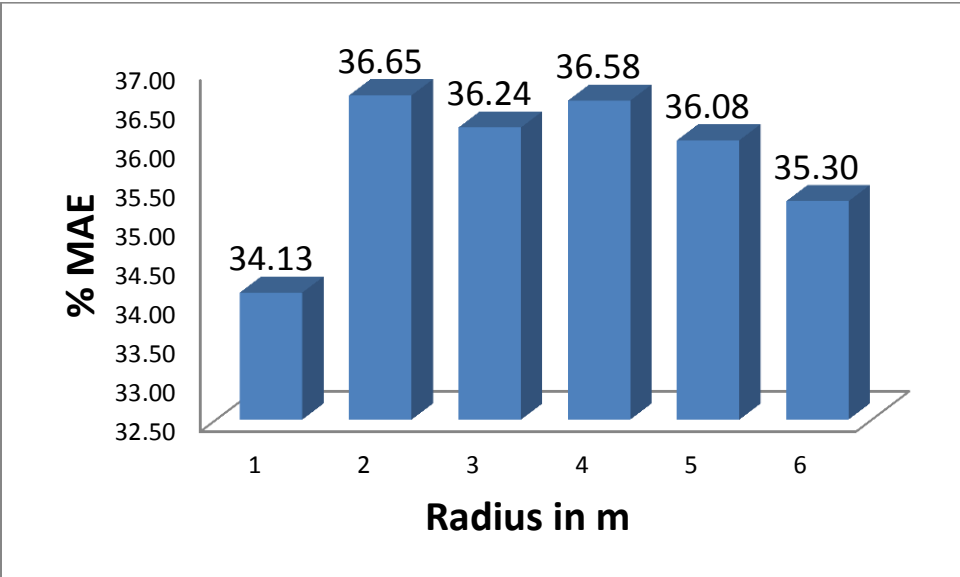
Figure 4.4. The Mean Absolute Error
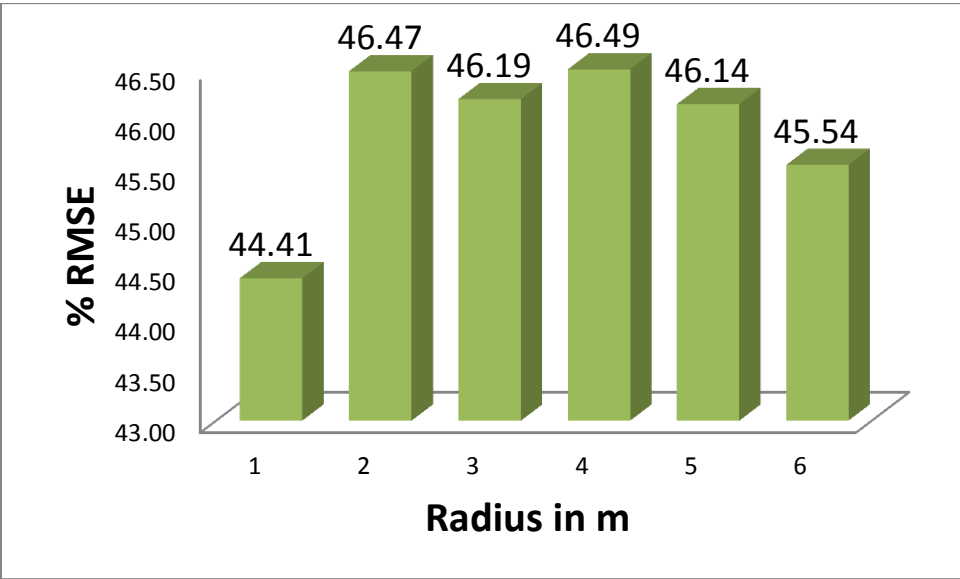
Figure 4.5. The Root Mean Squared Error
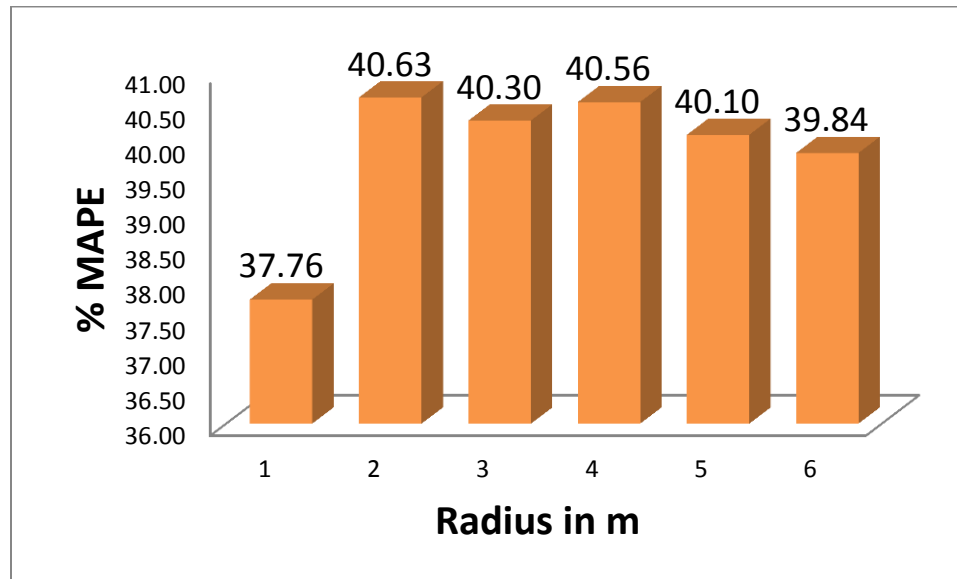
Figure 4.6. The Mean Absolute Percentage Error

The lowest values for the errors are 34.13% for the MAE, 44.41% for the RMSE and 37.76% for the MAPE. These are all obtained at a radius of 1 m. This is the minimum distance between the sampling points for the power density. Using more neighbors for the estimation resulted in larger errors. Therefore, this is the radius used to estimate the values needed for the map.

The map generated using Ordinary Kriging is shown in Figure 4.8. The unknown values are estimated every 0.1 m from the measured power densities illustrated in Figure 4.7 in order to produce a smoother map.
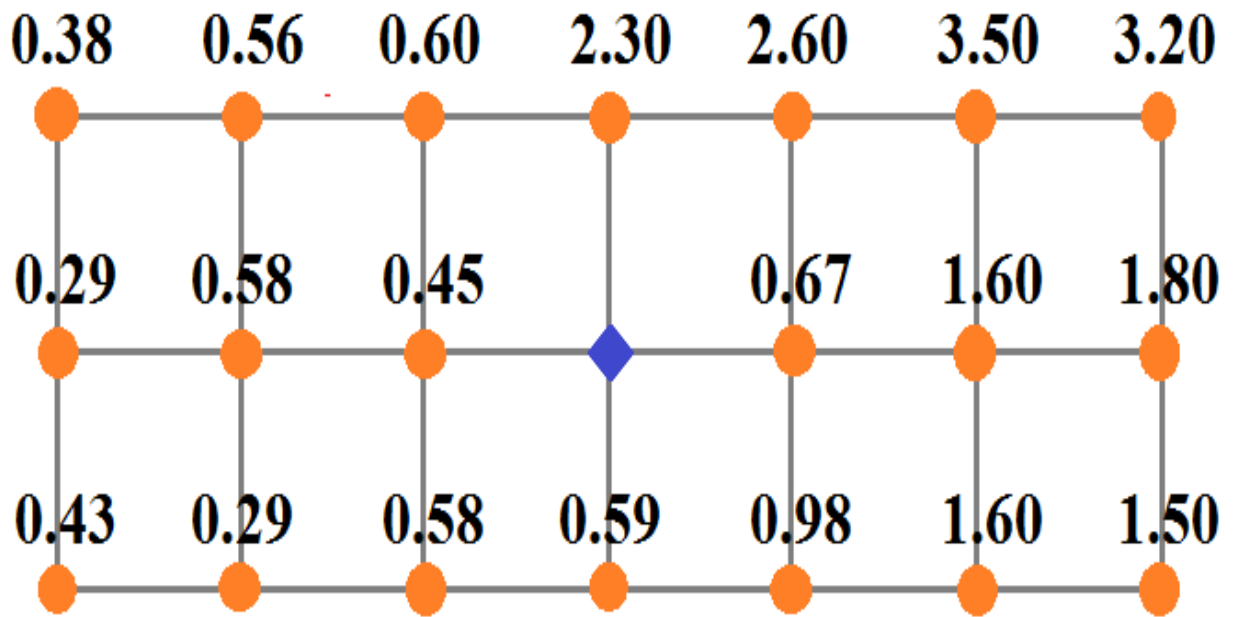
Figure 4.7. The Measured Power Densities in $\frac{mW}{m^2}$ Per Grid Point
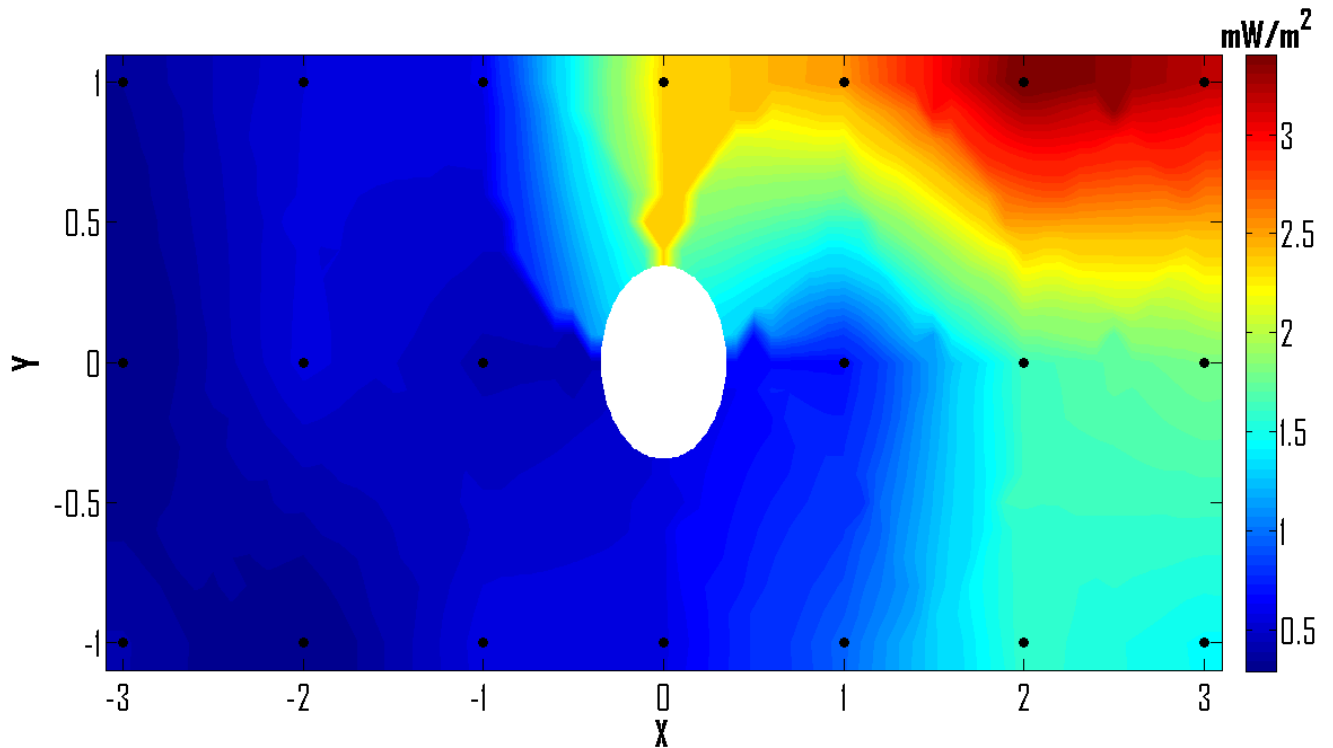
Figure 4.8. The Radiofrequency Map Generated From the Interpolated Power Densities.
The black dots indicate the actual sampling points.
The white area is occupied by the post where the antenna is mounted.

Since the source is an omnidirectional antenna, it should radiate equally in all directions theoretically. However, it can be seen from the generated radiofrequency map that this is not the case. This might be attributed to the multi-path interference and the reflections caused by the objects in the environment where the measurements are made [27]. Referring back to Figure 3.6, the signal is attenuated by the tree branches near the post. This is possibly the reason for the low values measured which are designated in the map as the dark blue regions.

CHAPTER 5

CONCLUSION AND RECOMMENDATIONS

Through the use of an interpolation method, the electromagnetic environment can be characterized with a fewer samples. This gives way to a more efficient and a faster sampling procedure to measure the power density levels. Radiofrequency maps are generated through this technique. These maps are easily comprehensible representations of the exposure to non-ionizing radiation which can be used as a tool for information dissemination.

Cross validation was performed in order to determine the optimal search radius for the interpolation. This was assessed through the computation of the Mean Error (ME), Root Mean Squared Error (RMSE) and the Mean Average Percentage Error (MAPE). The lowest errors are obtained using a radius of 1 m with a corresponding 34.13% ME, 44.41% RMSE and 37.76% MAPE.

The ODAS node installed with an omnidirectional antenna examined in this study complies with the exposure limits set by the ICNIRP. The highest value of the power density measured is only 0.07 % of the reference level for the exposure of the general public to radiofrequency radiation. Therefore, it can be concluded that the exposure from the measured antenna is very safe at the street level.

For future studies, a radiofrequency mapping of a whole ODAS can be considered. Broadband measurements that encompass all frequencies used by the antennas in the system can provide better understanding of its total contribution to the human exposure from non-ionizing radiation.

REFERENCES

[1] Ford, T. (2013). *Distributed Antenna Systems (DAS) and Small Cell Technologies Distinguished*. The HetNet Forum | The HetNet Builders' Online Community. Retrieved from http://www.thedasforum.org/wp-content/uploads/2014/07/DAS-and-Small-Cell-Technologies-Distinguished_HNForum.pdf

[2] Yu, X., Liu, X., Xin, Y., Chen, M., & Rui, Y. (2012). Capacity Analysis of Distributed Antenna Systems with Multiple Receive Antennas over MIMO Fading Channel. *International Journal Of Antennas And Propagation*, 2012, 1-7. doi:10.1155/2012/409254

[3] Ford, T. (2013). Installing DAS & Small Cells- What You Need To Know. *BISCI News Magazine*, (Volume 34, number 2). Retrieved from http://www.thedasforum.org/wp-content/uploads/2013/04/Ford-BISCI-News-Article.pdf

[4] Hu, H., Zhang, Y., & Luo, J. (2007). Distributed antenna systems. Boca Raton: Auerbach Publications.

[5] Bell, T. (2014). *PIM testing Distributed Antenna Systems: Which frequency band should I use? - Anritsu America. Anritsu.com*. Retrieved 27 November 2014, from http://www.anritsu.com/en-US/Events/Online-Webinars/2014/WBN002366.aspx

[6] Ford, T. (2014). Implications of Small Cells. *Mission Critical Communications*. Retrieved from http://www.thedasforum.org/wp-content/uploads/2014/08/Mission-Critical-Spectrum-low-res-8-14.pdf

[7] GMA News,. (2013). *Globe turns to fiber optics to boost mobile phone signal.* Retrieved from http://www.gmanetwork.com/news/story/318636/scitech/technology/globe-turns-to-fiber-optics-to-boost-mobile-phone-signal

[8] Cortel-Carrasco, A., Ould Isselmou, Y., Wong, M., & Wiart, J. Management of electromagnetic fields in the environment. International Union of Radio Science, France Telecom.

[9] Klauenberg, B., & Miklavčič, D. (2000). Radio frequency radiation dosimetry and its relationship to the biological effects of elecromagnetic fields. Dordrecht: Kluwer Academic Publishers.

[10] Beekhuizen, J. (2014). *Determining the validity of exposure models for environmental epidemiology: predicting electromagnetic fields from mobile phone base stations*. (Ph.D.). Utrecht University.

[11] Who.int,. (2015). *WHO | Electromagnetic fields and public health*. Retrieved 19 May 2015, from http://www.who.int/peh-emf/publications/facts/fs304/en/

[12] Baes, F. (2014). *Radiofrequency (RF) Radiation*. Hps.org. Retrieved 28 October 2014, from http://hps.org/hpspublications/articles/rfradiation.html

[13] Cember, H., & Johnson, T. (2009). *Introduction to health physics.* New York: McGraw-Hill Medical.

[14] Hengl, T. (2009). *A practical guide to geostatistical mapping*. [Amsterdam: Hengl].

[15] Resources.arcgis.com,. (2015). *ArcGIS Help 10.1*. Retrieved 9 May 2015, from http://resources.arcgis.com/en/help/main/10.1/index.html#//00310000023000000

[16] Li, J., & Heap, A. (2008). *A Review of Spatial Interpolation Methods for Environmental Scientists* (pp. 10-15). Geoscience Australia.

[17] Aerts, S., Deschrijver, D., Verloock, L., Dhaene, T., Martens, L., & Joseph, W. (2013). Assessment Of Outdoor Radiofrequency Electromagnetic Field Exposure Through Hotspot Localization Using Kriging-Based Sequential Sampling. *Environmental Research*, *126*, 184-191. doi:10.1016/j.envres.2013.05.005

[18] Ureten, S., Yongaçoglu, A., & Petriu, E. (2012). A Comparison Of Interference Cartography Generation Techniques In Cognitive Radio Networks. In *IEEE International Conference on Communications* (pp. 1879-1883). Ottawa: IEEE.

[19] Paniagua, J., Rufo, M., Jimenez, A., & Antolin, A. (2011). The Spatial Statistics Formalism Applied To Mapping Electromagnetic Radiation In Urban Areas. *Environmental Monitoring And Assessment*, *185*, 311-322. doi:10.1007/s10661-012-2555-7

[20] Oliver, M., & Webster, R. (2014). A Tutorial Guide To Geostatistics: Computing And Modelling Variograms And Kriging. *CATENA*, *113*, 56-69. doi:10.1016/j.catena.2013.09.006

[21] ICNIRP Guidelines for limiting exposure to time-varying, electric, magnetic and electromagnetic fields (up to 300 GHz). (1998). Health Physics, 74(4).

[22] Vanhoy, G., Volos, H., Bastidas, C., & Bose, T. (2013). A Spatial Interpolation Method for Radio Frequency Maps Based on the Discrete Cosine Transform. MILCOM 2013 - 2013 IEEE Military Communications Conference. doi:10.1109/milcom.2013.181

[23] Robinson, T., & Metternicht, G. (2006). Testing the performance of spatial interpolation techniques for mapping soil properties. *Computers And Electronics In Agriculture*, 50(2), 97-108. doi:10.1016/j.compag.2005.07.003

[24] Yao, X., Fu, B., Lü, Y., Sun, F., Wang, S., & Liu, M. (2013). Comparison of Four Spatial Interpolation Methods for Estimating Soil Moisture in a Complex Terrain Catchment. *Plos ONE*, 8(1), e54660. doi:10.1371/journal.pone.0054660

[25] Ramm, J. (2011). Kriging and Inverse Distance Interpolation Using Gstat [Computer Program]. Retrieved from http://www.sourcecodeonline.com/details/kriging_and_inverse_distance_interpolation_using_gstat.html

[26] Schwanghart, W. (2010). Variogramfit [Computer Program]. Retrieved from http://www.sourcecodeonline.com/details/variogramfit.html

[27] Office of Engineering and Technology, Federal Communications Commission,. (1997). *Evaluating Compliance with FCC Guidelines for Human Exposure to Radiofrequency Electromagnetic Fields*. Washington, D.C. 20554.

[28] Base Station Antennas. (1st ed., p. 14). Retrieved from http://www.rosenberger.com/cn_en/publication/pdf/BaseStationAntennas.pdf

[29] DAS Distributed Antenna Systems: A Safe Solution For Meeting The Wireless Coverage Needs Of Your Community. (2015) (1st ed., p. 2). Retrieved from http://www.americantower.com/Assets/uploads/files/PDFs/Americantower_DAS_safety_brochure.pdf

[30] Narda Safety Test Solutions. Selective Measurement of High Frequency Electric and Magnetic Fields. Retrieved from http://www.narda-sts.com

APPENDIX A:

CALIBRATION CERTIFICATE OF NARDA SRM-3000

Narda Safety Test Solutions GmbH
Sandwiesenstrasse 7 - 72793 Pfullingen - Germany
Phone: +49 7121 9732 0 - Fax: +49 7121 9732 790

narda
Safety Test Solutions®
an (E) Communications Company

Calibration Certificate

Narda Safety Test Solutions hereby certifies that the object referred to in this certificate has been calibrated by qualified personnel using Narda's approved procedures. The calibration was carried out in accordance with a certified quality management system which conforms to ISO 9001

OBJECT	Antenna, Three-Axis, E-Field, 27 MHz to 3 GHz
MANUFACTURER	Narda Safety Test Solutions GmbH
PART NUMBER (P/N)	3501/03
SERIAL NUMBER (S/N)	K-0015
CUSTOMER	
CALIBRATION DATE	2014-01-31
RESULT ASSESSMENT	within specifications
AMBIENT CONDITIONS	Temperature: (23 ± 3) °C Relative humidity: (20 to 60) %
CALIBRATION PROCEDURE	3000-8702-00A

MANAGEMENT SYSTEM

ISSUE DATE: 2014-01-31

CALIBRATED BY
Rilling

AUTHORIZED SIGNATORY

Certified by DQS against
ISO 9001:2008
(Reg.-No. 099379 QM08)

This calibration certificate may not be reproduced other than in full except with the permission of the issuing laboratory. Calibration certificates without signature are not valid.

Narda Safety Test Solutions GmbH
Sandwiesenstrasse 7 - 72793 Pfullingen - Germany
Phone: +49 7121 9732 0 - Fax: +49 7121 9732 790

narda
Safety Test Solutions®
an (B) Communications Company

OBJECT

The sensor mechanism comprises three dipoles in an orthogonal (mutually perpendicular) arrangement.
The received signal of each dipole is in turn switched to the output of the object. Control of the built-in multiplexer is achieved by the SRM basic unit via the control cable.

CALIBRATION PROCEDURE

The calibration of the object was performed in the frequency domain using an unmodulated (CW) signal. The measurement involved the generation of a linearly polarized electromagnetic field, approximating to a plane wave, into which the object was placed.

SETUP A (1800 MHz to 3 GHz)

Calibration using the transfer standard. Pyramidal standard gain horn antennas are mounted in a microwave anechoic chamber. During adjustment of the setup the power P.ref had been transmitted while the reference standard was indicating the field strength E.ref
During calibration of the object the field strength was set to an allowed value calculated from the actual power meter reading P.m .

$$E_{actual} = E_{ref} \cdot \sqrt{P_m / P_{ref}}$$

The object was positioned with the bore sight of the horn at a distance of 0.7 m with its handle oriented in the ortho-angle (54°) to the vertical E-field. The beaming direction varied from -45° to +45° in reference to the PE-PS-plane, depending on the horn used in specific frequency band.

SETUP B (200 MHz to 1800 MHz)

Calibration using the transfer standard. A broadband double ridged waveguide horn is mounted in a microwave anechoic chamber. During adjustment of the setup the power P.ref had been transmitted while the reference standard was indicating the field strength E.ref
During calibration of the object the field strength was set to an allowed value calculated from the actual power meter reading P.m .

$$E_{actual} = E_{ref} \cdot \sqrt{P_m / P_{ref}}$$

The object was positioned with the bore sight of the horn at a distance of 1 m with its handle oriented in the ortho-angle (54°) to the vertical E-field.

SETUP D (9 kHz to 100 MHz)

Calibration using calculated field strength. A Crawford TEM cell is used to generate the known field strength E. The field strength is derived from TEM cell's septum height b, impedance Z0 and from the output power of the cell. The output power measurement includes the power meter's response Pm Fth and a fixed attenuation D.

$$E = \frac{\sqrt{P_m \cdot F_{th} \cdot D \cdot Z_0}}{b}$$

The object was positioned with its handle oriented in the ortho-angle (54°) to the vertical E-field.

narda
Safety Test Solutions®
an ⓔ Communications Company

MEASUREMENT

The output voltage U of the object was measured with a power sensor that was connected via a ferrite-beaded coaxial cable. The insertion loss of this cable was taken into account during the measurement.

For each frequency the object had been rotated about the axis of the handle by 60° and then stopped to record the output voltage of each axis separately. (At every 120° position one dipole axis was aligned with the incident field vector). At each stop the resultant voltage was calculated from the three-axis values:

$$U_i = \sqrt{U_x^2 + U_y^2 + U_z^2}$$

After a full revolution of 360° had been made the results were calculated from the recorded voltage as follows

ANTENNA FACTOR

The antenna factor AF was calculated at each frequency:

$$AF_{actual} = 20 \log\left(\frac{E_{actual}/U_{mean}}{1/m}\right) dB(1/m)$$

with

$$U_{mean} = \sqrt{Min(U_i)\,Max(U_i)}$$

ISOTROPY

The anisotropy is defined as

$$A = 20 \log\left(Max(U_i)/\sqrt{Min(U_i)\,Max(U_i)}\right) dB$$

DEVIATION

The deviation since the last calibration and adjustment is calculated as follows:

$$Deviation = \left(AF_{memory} - AF_{actual}\right)$$

The values AF.memory were uploaded from the memory chip at receipt of antenna. These values represent the results of the former calibration.

METROLOGICAL TRACEABILITY

The calibration results are traceable to National Standards, which are consistent with the recommendations of the General Conference on Weights and Measure (CGPM), or to standards derived from natural constants. Physical units, which are not included in the list of accredited measured quantities such as field strength or power density, are traced to the basic units via approved measurement and computational methods.

The equipment used for this calibration is traceable to the reference listed above and the traceability is guaranteed by ISO 9001 Narda internal procedure.

STANDARD	MANU FACTURER	MODEL	SERIAL NUMBER	CERTIFICATE	NEXT CAL. DATE	TRACE
Power Sensor	R&S	NRV-Z4	100122	0277 D-K-15195-01-00 2012-04	2014-04	DAkkS
RF-Millivoltmeter	R&S	URV55	100213	0253 D-K-15195-01-00 2012-08	2014-08	DAkkS
SETUP A (1800 MHz to 3 GHz)						
E-Field Reference Probe	Narda	EF1891	A-0093	2012100100-1R	2014-11	UKAS 0478
SETUP B (200 MHz to 1600 MHz)						
E-Field Reference Probe	Narda	EF1891	A-0093	2012100100-1R	2014-11	UKAS 0478
SETUP D (100 kHz to 100 MHz)						
Calliper	Preisser	0-800mm	310121016	1183737 DKD-K-12001 2011-03	#	DKD
RF-Millivoltmeter	R&S	URV55	100627	0222 D-K-15195-01-00 2012-10	2014-10	DAkkS
Power Sensor	R&S	NRV-Z51	101777	0360 D-K-15195-01-00 2012-12	2014-12	DAkkS
Attenuator	Weinschel	49-30-33	KC115	220851 D-K-15012-01-00 2011-07	2014-07	DAkkS

Reference standard; not used for routine calibration

UNCERTAINTY

The uncertainty stated in this document is the expanded uncertainty with a coverage factor of 2 (corresponding, in the case of normal distribution, to a confidence probability of 95%).

The uncertainty analysis for this calibration was done in accordance with the ISO-Guide (Guide to the expression of Uncertainty in Measurement). The uncertainties are derived from contributions from the measurement of power, impedance, attenuation, mismatch, length, frequency, stability of instrumentation, repeatability of handling and field uniformity in the field generators (TEM cell and anechoic chamber).

This statement of uncertainty applies to the measured values only and does not make any implementation or include any estimation as to the long-term stability of the calibrated device.

narda
Safety Test Solutions®
an (E) Communications Company

RESULTS

These results describe the uncorrected frequency response of the object.

Frequency Response   **passed**

Frequency in MHz	E_actual in V/m	U_mean in dB(µV)	Uncertainty in dB	AF_actual in dB(1/m)	Deviation in dB
26	10,0	70,90	1,0	69,10	-0,08
45	10,0	74,76	1,0	65,24	-0,03
75	10,0	78,89	1,0	61,11	-0,06
100	10,0	80,79	1,0	59,21	-0,07
200	10,0	85,47	1,0	54,53	0,59
300	10,0	87,81	1,0	52,19	0,19
433	10,0	88,97	1,5	51,03	0,99
600	10,0	90,48	1,5	49,52	-0,24
750	10,0	90,96	1,5	49,04	0,12
900	10,0	91,58	1,5	48,42	-0,16
1000	10,0	91,82	1,5	48,18	0,06
1200	10,0	92,10	1,5	47,90	0,24
1400	10,0	91,99	1,5	48,01	1,04
1600	10,0	92,55	1,5	47,45	1,84
1800	10,0	91,14	1,0	48,86	-0,07
2000	10,0	90,14	1,0	49,86	0,57
2200	10,0	87,91	1,0	52,09	-0,13
2450	10,0	85,46	1,0	54,54	-0,29
2700	10,0	83,64	1,0	56,36	-0,66
3000	10,0	82,01	1,0	57,99	-0,24

Frequency Flatness (100 - 3000 MHz):   11,8 dB

Note: The result *AF_actual* is stored in the memory chip and will automatically be operative when the antenna is connected to a SRM basic unit to measure field strength.

Three-Axis E-Field Antenna SRM

36

narda
Safety Test Solutions®
an (L) Communications Company
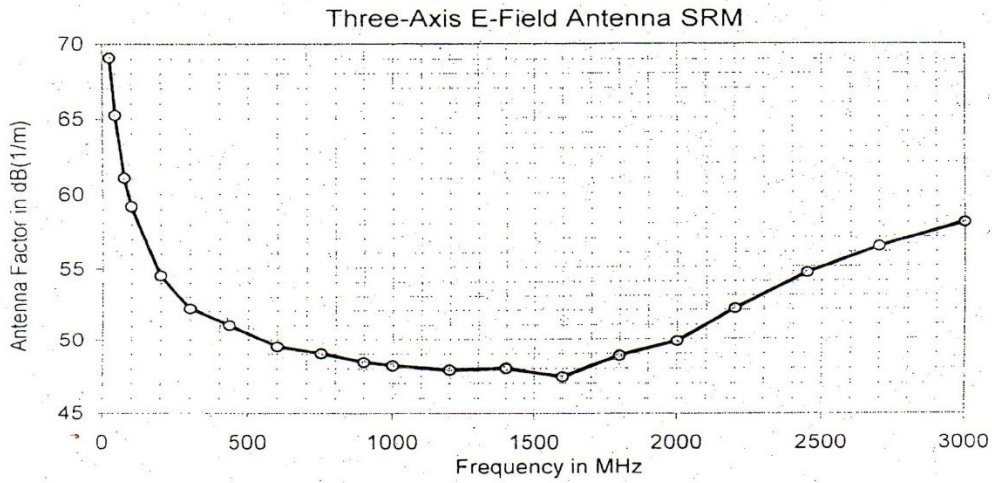
Isotropy   passed

Frequency in MHz	A in dB
26	0,18
45	0,13
75	0,12
100	0,14
200	0,20
300	0,22
433	0,21
500	0,25
750	0,25
800	0,26
1000	0,34
1200	0,36
1400	0,37
1600	0,61
1800	0,67
2000	0,74
2200	0,91
2450	1,06
2700	1,48
3000	1,84

Output Return Loss   passed

ANTENNA SPECIFICATIONS

Omni-Directional 870-960MHz 11dBi

Part Number	S-Wave 09-OD-11-F
Electrical Specifications	
Frequency Range	870-960MHz
Polarization	Vertical
Gain	11dBi
Horizontal 3dB Beam Width	360
Vertical 3dB Beam Width	7.5º
Electrical Down Tilt	0º, Fixed
Impedance	50Ω
VSWR	＜ 1.5
Max, Power Per Input	500W
Mechanical Specifications	
Connector Type	1 X 7-16 DIN(F)
Weight	7.5kg
Max. Wind Velocity	200Km/h
Dimension	Ø65 X 3560mm
Radome Material	Fiberglass
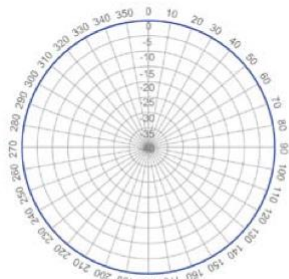
Horizontal Pattern   Vertical Pattern

870~960
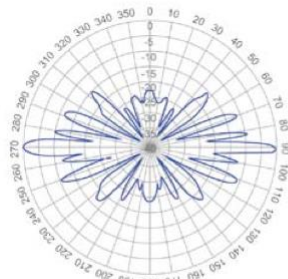
7-16 DIN

APPENDIX C:

REQUEST LETTERS

Cover of the Letter of Request to Globe Telecom Inc.

Republic of the Philippines
Department of Health
Food and Drug Administration
CENTER FOR DEVICE REGULATION, RADIATION HEALTH, AND RESEARCH
(former name: Bureau of Health Devices and Technology)

February 4, 2015

Mr. Ashish Pilani
Head, Wireless Engineering & Implementation
Network Technical Group
Globe Telecom, Inc.
Bonifacio Global City, Taguig

RE: Permission to Conduct Research Study on Outdoor Distributed Antenna System (ODAS)

Dear **Mr. Pilani:**

The Center for Device Regulation, Radiation Health, and Research (CDRRHR) of the Food and Drug Administration of the Department of Health is the national government agency with regulatory functions over radiation devices and facilities.

CDRRHR and the University of the Philippines-Manila will undertake a research project concerning non-ionizing radiation protection. The joint research team will take measurements of radiofrequency/microwave radiation levels of your ODAS installation at Dasmariñas Village, Makati. Measurement locations will be identified using a pre-determined grid (Annex A). The data gathering will be within the period of February 2015 to July 2015. We will provide your office a copy of the results.

Attached as Annex B is the list of persons who will be involved in the data-gathering. Annex C is also included which indicates the information we would like to obtain from your office. Please contact Ms. Mayneth Vince R. Oftana through her phone number (09369818636) or her email address (maynethvince@gmail.com) for more information.

We look forward to your cooperation as we work together towards ensuring radiation protection for our people.

Very truly yours,

Agnette P. Peralta, MSc
Director IV, CESO III

Building 24, San Lazaro Compound, Rizal Avenue, Sta. Cruz, 1003 Manila Telefax Nos. (632)711-60-16
(632)711-68-24; Trunk Line: (632) 651-78-00 locals 3401, 3402, 3403, 3404, 3405; 3408, 3409, 3410, 3411
E-mail: apperalta@fda.gov.ph; apperalta@co.doh.gov.ph, Website: www.doh.gov.ph

39

Cover of the Letter of Request to Homeowner's Association of Dasmariñas Village

Department of Physical Sciences and Mathematics
College of Arts and Sciences
University of the Philippines Manila

March 20, 2015

Mr. Mamerto R. Rodriguez
Village Manager

ATTN: Romy V. Cruz

Re: Research Study on Outdoor Distributed Antenna System

Dear **Mr. Rodriguez:**

I am Randy Fernandez, a full-time instructor of the University of the Philippines Manila. This letter is in response to our previous visit wherein we were requested to submit the list of people involved for our research study.

Our research team will be conducting our study on March 25 (Wednesday) and 26 (Thursday), from 8:00 am to 5:00 pm. We will be measuring the signal strength and radiation levels emitted by the antennas installed by Globe Telecom in your village. Data gathered from this measurement will be analyzed and submitted as a research on Outdoor Distributed Antenna Systems (ODAS). We will also provide a copy of the results to your office.

Attached herewith are the following:
- methodology to be used for data measurement
- list of personnel involved in the study
- list of vehicles and equipment to be used
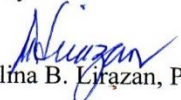
If you have further questions, please feel free to contact Ms. Mayneth Oftana through the information below or through her number (+63 936 981 8636) or email address (maynethvince@gmail.com).

Sincerely yours,

Randy Joseph G. Fernandez
Faculty

Noted by:

Marcelina B. Lirazan, Ph.D.
Chair

Telefax no. 254-18-81; Trunkline no. 516-32-28 loc. 118; Email: dpsm-cas@upm.edu.ph
Rm. 102 Rizal Hall Bldg., P. Faura St., Ermita 1000, Manila

Letter of Request to the Department of Health

April 24, 2015

Engineer Maria Gladys R. Cabrera, MSc.
Health Physicist IV
Chief, Radiation Regulation Division

RE: Assistance of DOH in radiation survey at Dasmariñas Village, Makati

Dear **Engr. Cabrera:**

I am Mayneth Vince Oftana, a graduating BS Applied Physics (Health Physics) student of the University of the Philippines 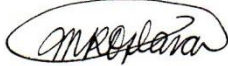Manila. My special problem is about the exposure of the general public from the radiofrequency radiation of the Outdoor Distributed Antenna System (ODAS) installed at Dasmariñas Village in Makati. Thus, I would like to request for the assistance my advisers, namely Ms. Realyn Joy Uy, MSc. and Ms. Annie Lorraine Joyas, MSc. in conducting measurements on the different areas around the village. I would also like to ask for permission to use the Narda SRM-3000 for this matter.

Should your office need more information, I am available through my phone number (09369818636) or e-mail address (maynethvince@gmail.com).
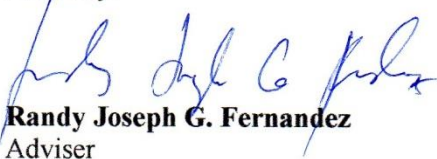
Thank you very much and hoping for your kind consideration.

Sincerely yours,

Mayneth Vince R. Oftana
Student, BS Applied Physics

Noted by:

Randy Joseph G. Fernandez
Adviser

APPENDIX D

RAW DATA

Table A.1 The Measured Power Density Per Sampling Point in the Grid with GPS Location

Measurement Point	Data Table As Saved in Narda	Measured Power Density		GPS Location	
(-3,1)	327.1	380.0	μW/m^2	N 14^{0}32.088'	E 121^{0}01.692'
(-2,1)	328.1	556.4	μW/m^2	N 14^{0}32.088'	E 121^{0}01.690'
(-1,1)	329.1	604.5	μW/m^2	N 14^{0}32.082'	E 121^{0}01.692'
(0,1)	330.1	2.346	mW/m^2	N 14^{0}32.085'	E 121^{0}01.692'
(1,1)	331.1	2.560	mW/m^2	N 14^{0}32.086'	E 121^{0}01.690'
(2,1)	332.1	3.450	mW/m^2	N 14^{0}32.089'	E 121^{0}01.690'
(3,1)	333.1	3.224	mW/m^2	N 14^{0}32.088'	E 121^{0}01.691'
(3,0)	334.1	1.805	mW/m^2	N 14^{0}32.083'	E 121^{0}01.695'
(2,0)	335.1	1.641	mW/m^2	N 14^{0}32.087'	E 121^{0}01.696'
(3,-1)	336.1	1.479	mW/m^2	N 14^{0}32.086'	E 121^{0}01.699'
(2,-1)	337.1	1.611	mW/m^2	N 14^{0}32.091'	E 121^{0}01.694'
(1,-1)	338.1	984.3	μW/m^2	N 14^{0}32.091'	E 121^{0}01.693'
(1,0)	339.1	676.4	μW/m^2	N 14^{0}32.089'	E 121^{0}01.694'
(0,-1)	340.1	590.2	μW/m^2	N 14^{0}32.086'	E 121^{0}01.691'
(-1,-1)	341.1	583.6	μW/m^2	N 14^{0}32.083'	E 121^{0}01.693'
(-1,0)	342.1	452.2	μW/m^2	N 14^{0}32.082'	E 121^{0}01.694'
(-2,0)	343.1	576.3	μW/m^2	N 14^{0}32.082'	E 121^{0}01.694'
(-2,-1)	344.1	289.6	μW/m^2	N 14^{0}32.085'	E 121^{0}01.694'
(-3,-1)	345.1	428.8	μW/m^2	N 14^{0}32.085'	E 121^{0}01.698'
(-3,-0)	346.1	289.7	μW/m^2	N 14^{0}32.088'	E 121^{0}01.698'

APPENDIX E

SOURCE CODE

```
%This is the source code used for the interpolation and cross
%validation of the measured power density values.
%The functions used are as follows:
%   SampleVarioGstat and InterpolationGstat by James Ramm [25]
%   variogramfit by Wolfgang SchwangHart [26]



%The measured power densities with their corresponding location
%following the sampling grid are inputted as the matrix "data"

data = [
     -3 1 .380
     -2 1 .5564
     -1 1 .6045
      0 1 2.346
      1 1 2.560
      2 1 3.45
      3 1 3.224
     -3 0 .2897
     -2 0 .5763
     -1 0 .4522
      1 0 .6764
      2 0 1.641
      3 0 1.805
     -3 -1 .4288
     -2 -1 .2896
     -1 -1 .5836
      0 -1 .5902
      1 -1 .9843
      2 -1 1.611
      3 -1 1.479
];

x = data(:,1); %x location
y = data(:,2); %y location
z = data(:,3); %Measured power density in mW/m2


%Computation of the Experimental Variogram
lag=1;
maxdist=7;
[av_dist,gamma,h,np]=SampleVarioGstat(x,y,z,lag,maxdist);

%Fitting the Experimental Variogram Into A Linear Model
%The linear model is used since it provides a good fit to the measured
%values
c0 = max(gamma);
a0 = max(h)*2/3;
[a,c,n,S] = variogramfit(h,gamma,a0,c0,np,'model', 'blinear');
```

```matlab
%Interpolation of the Values
res=0.1;
radius =1;
[xi,yi,zi]=InterpolationGstat(x,y,z,res,radius,'kriging',0,'intval',S);

%Printing the Values Obtained From the Interpolation
[m,n]=size(zi);
fileID=fopen('Results.txt','wt');
fprintf(fileID,'%6s %24s %24s \n','xi','yi','zi');
for i=1:(m*n)
    fprintf(fileID,'%6.2f %18.2f %18.4f \n',xi(i),yi(i),zi(i));
end
fclose(fileID);

%Mapping the Interpolated Values
[c,lines]=contourf(xi,yi,zi,70);
set(lines,'linestyle','none');
colorbar;
hold on
scatter(x,y,50,'o','k','filled');

%Indicating the Antenna in the Radiofrequency Map
rad=0.345;
th=0:pi/50:2*pi;
xunit=rad*cos(th)+0;
yunit=rad*sin(th)+0;
fill(xunit,yunit,'w','Edgecolor','none');
hold off
```

APPENDIX F

CROSS-VALIDATION

Table A.2. Interpolated Values Using Different Search Radii

x	y	z	Interpolated Values Using Different Search Radii					
			1m	2m	3m	4m	5m	6m
-3	1	0.38	0.423	0.407	0.4587	0.4749	0.5084	0.5107
-2	1	0.5564	0.5114	0.5049	0.5114	0.5384	0.5338	0.6499
-1	1	0.6045	1.2247	1.2219	1.2746	1.2837	1.2818	1.2818
0	1	2.346	1.5825	1.3733	1.3742	1.3823	1.3823	1.3823
1	1	2.56	2.3946	2.4034	2.4202	2.4195	2.42	2.42
2	1	3.45	2.6086	2.6049	2.6192	2.6202	2.6189	2.6185
3	1	3.224	2.6275	2.7306	2.8165	2.7434	2.7877	2.8661
-3	0	0.2897	0.4434	0.4503	0.4383	0.423	0.4153	0.4244
-2	0	0.5763	0.397	0.396	0.3396	0.3267	0.4217	0.4203
-1	0	0.4522	0.5903	0.7675	0.7087	0.6583	0.6606	0.6606
1	0	0.6764	1.7423	1.675	1.679	1.6766	1.6768	1.6768
2	0	1.641	1.8855	1.8837	1.8903	1.8962	1.8792	1.8283
3	0	1.805	2.1905	2.271	2.2512	2.2558	2.2593	2.2612
-3	-1	0.4288	0.29	0.2594	0.2664	0.2263	0.2533	0.4953
-2	-1	0.2896	0.5222	0.5209	0.4799	0.4938	0.5143	0.5459
-1	-1	0.5836	0.4427	0.4275	0.4059	0.3852	0.3848	0.3848
0	-1	0.5902	0.784	0.7343	0.6935	0.6954	0.6954	0.6954
1	-1	0.9843	1.0043	0.883	0.8574	0.8584	0.8644	0.8644
2	-1	1.611	1.3243	1.1925	1.149	1.1635	1.1517	1.1787
3	-1	1.479	1.708	1.6949	1.6585	1.6443	1.6693	1.6686

These are the values obtained through interpolation of the measured power density "z" using varied search radii. Cross-validation was performed by obtaining the ME, RMSE and MAPE from these values.